Exp.-Nr. A2/ 1-03
Eingang:
an PAC:

Mainz Microtron MAMI

Collaboration A2: "Real Photon Experiments"
Spokesperson: R. Beck

Proposal for an Experiment

Measurement of the Magnetic Dipole Moment of the $\Delta^+(1232)$-Resonance via the $\gamma + p \to n + \pi^+ + \gamma'$ reaction

Collaborators:
CrystalBall@MAMI collaboration
Spokespersons for the Experiment: D.P. Watts - Edinburgh ; G. Rosner - Glasgow.

Abstract of Physics:
We propose to determine the magnetic dipole moment of the $\Delta^+(1232)$ resonance from measurements of the five-fold differential cross section for the reaction $\gamma + p \to n + \pi^+ + \gamma'$ in the region of the Δ resonance ($E_\gamma = 300 - 500$ MeV) and the photon asymmetry Σ for linearly polarized photons. The data will be obtained at the same time as that of the $\gamma + p \to p + \pi^0 + \gamma'$ reaction which already has PAC approval. We require a beam of tagged polarized photons incident on a liquid hydrogen target. The π^+, γ' and n final state particles are measured with the Crystal Ball large acceptance multiphoton spectrometer with TAPS as forward-wall detector. A combination of central tracker and particle ID detector will be used to identify and measure the trajectory of the π^+ in the ball.

Abstract of Equipment:
We require a beam of tagged linearly polarized photons incident on a liquid hydrogen target and the detection of the three final state particles. The Glasgow tagging system will provide the intense, linearly polarized photon beam. The Crystal Ball 4π spectrometer in combination with TAPS as forward wall will be used to measure the π^+, γ and n in the final state.

MAMI–Specifications:

beam energy	880 MeV
beam current	< 100 nA
time structure	cw
polarization	linearly polarised photons

Experiment–Specifications:

experimental hall/beam	A2
detector	Crystal Ball and TAPS as forward wall
target material	liquid hydrogen

Beam Time Request:

set–up without beam	Crystal Ball and TAPS initial setup time ($\approx$ 3 mo.)
set–up/tests with beam	300 hours (parallel with proposal A2/ 1-02)
data taking	600 hours (parallel with proposal A2/ 1-02)

Title: **Measurement of the Magnetic Dipole Moment of the $\Delta^+(1232)$ Resonance via the $\gamma p \to \gamma' \pi^+ n$ reaction**

Participants: J. Brudvik, B.M.K. Nefkens, S.N. Prakhov, J.W. Price, and A. Starostin
University of California, Los Angeles, CA, USA

J. Ahrens, H.J. Arends, R. Beck, D. Drechsel, D. Krambrich, M. Lang, S. Scherer, S. Schumann, A. Thomas, L. Tiator, M. Unverzagt, D. von Harrach and Th. Walcher
Institut für Kernphysik, University of Mainz, Germany

S. Altieri, A. Braghieri, P. Pedroni, and T. Pinelli
INFN Sezione di Pavia, Pavia, Italy

J.R.M. Annand, R. Codling, E. Downie, D. Glazier, K. Livingston, J.C. McGeorge, I.J.D. MacGregor, D. Protopopescu and G. Rosner
Department of Physics and Astronomy, University of Glasgow, Glasgow, UK

C. Bennhold and W. Briscoe
George Washington University, Washington, USA

KS. Cherepnya, L. Fil'kov, and V. Kashevarow
Lebedev Physical Institute, Moscow, Russia

B. Boillat, M. Kotulla and B. Krusche, Institut für Physik
University of Basel, Basel, Ch

R. Gregor, V. Metag, S. Lugert, R. Novotny, M. Pfeiffer and S. Schadmand
II. Physikalisches Institut, University of Giessen, Germany

D. Branford, K. Foehl, C.M. Tarbert and D.P. Watts
School of Physics, University of Edinburgh, Edinburgh, UK

V. Lisin, R. Kondratiev and A. Polonski
Institute for Nuclear Research, Moscow, Russia

G.O'Reilly
University of Massachusetts, Dartmouth, USA

D. Hornidge
Mount Allison University, Sackville, Canada

P. Grabmayr and T. Hehl
Physikalisches Institut Universität Tübingen, Tübingen, Germany

H. Staudenmaier
Universität Karlsruhe, Karlsruhe, Germany

M. Manley
Kent State University, Kent, USA

M. Korolija and I. Supek
Rudjer Boskovic Institute, Zagreb, Croatia

T.D.S. Stanislaus
Valparaiso University, Valparaiso, USA

D. Sober
Catholic University, Washington DC

M. Vanderhaeghen
College of William and Mary, Williamsburg, USA

Spokespersons: D.P. Watts, Univ. of Edinburgh
email: daniel.watts@ph.ed.ac.uk
tel: +44 131 650 5256

G. Rosner, Univ. of Glasgow
email: g.rosner@physics.gla.ac.uk
tel: +44 141 330 2774q

We propose to determine the magnetic dipole moment of the $\Delta^+(1232)$ resonance from measurements of the five-fold differential cross section for the reaction $\gamma p \to \gamma' \pi^+ n$ in the region of the Δ resonance ($E_\gamma = 300 - 500$ MeV) and the photon asymmetry Σ. We require a beam of tagged linearly polarized photons incident on a liquid hydrogen target. The π^+, γ' and n final state particles are measured with the Crystal Ball large acceptance spectrometer with TAPS as forward-wall detector. Wire chambers and a thin plastic scintillator barrel will be used to measure the trajectory of and identify the π^+.

1 Introduction

The magnetic dipole moment, μ_b, of a baryon is due to the quark spins and to the average of the quark currents. As such the numerical value of μ_b is a fundamental characteristic of every baryon and provides us with a simple, elegant and sensitive way for testing the validity of the theoretical hadron description in the non-perturbative sector of QCD. This includes quark soliton models, the standard quark models, various effective Lagrangians and lattice QCD calculations. A knowledge of μ_b provides valuable additional information to the nuclear structure functions which are being probed with very high energy leptons as μ_b gives information on the quark correlations which are not measured in the lepton experiments.

For long lived particles μ_b is measured by precession in a magnetic field and this technique has been used to obtain the magnetic moment of p, n, Λ, *etc.* However the short mean-life of the Δ resonance precludes using this method. Instead we can take advantage of the very short lifetime (which implies a large width) by exploiting the Δ radiative decay to itself. This method has been successfully pioneered for the Δ^{++} using the pion induced reaction $\pi^+ p \to \Delta^{++} \to \gamma' \Delta^{++} \to \gamma' \pi^+ p$ [1].

We propose to measure the real photon induced reaction

$$\gamma p \to \Delta^+ \to \gamma' \Delta^+ \to \gamma' \pi^+ n \tag{1}$$

which is predicted[2] to show sensitivity to μ_{Δ^+}. The measurement will be obtained using the same beamtime as a similar experiment which exploits the $\gamma p \to \Delta^+ \to \gamma' \Delta^+ \to \gamma' \pi^0 p$ reaction and which has already obtained PAC approval. The simultaneous determination of both channels is extremely desirable as the background mechanisms to the Δ radiative decay in the two cases are very different. A theoretical description of the $\gamma p \to \gamma' \pi^+ n$ reaction presently exists, based on the approach described in Ref.[3]. A unitarized simultaneous description of both $n\pi^+\gamma'$ and $p\pi^0\gamma'$ reactions is expected to be available in the near future.

The $n\pi^+\gamma'$ cross section is small, having a value of $\sim 100nb$ integrated over decay photon energies in the region of interest above 50 MeV (Fig. 2). The measurement therefore relies on the intense, tagged, linearly polarized photon beam provided at MAMI-B by the Glasgow tagger. A thin diamond crystal radiator will produce linearly polarized photons via coherent bremsstrahlung. A large acceptance photon and hadron spectrometer is provided by the Crystal Ball using TAPS as a forward wall detector (CBTAPS). The neutron and π^+ detection capabilities of the CBTAPS system are discussed in sections 3.3 and 3.2.

Sufficient statistics can be obtained in the same beam time period approved for the $\gamma p \to \gamma' \pi^0 p$ reaction ie. production run of 500 hours.

2 Theoretical background to $\Delta(1232)$ Static Magnetic Dipole Moment Determination

If SU(6) symmetry holds, then the nucleon and the Δ resonance are degenerate and their magnetic moments are related through $\mu_\Delta = e_\Delta \, \mu_p$, where e_Δ is the ratio of the electric charges of the Δ and proton, and μ_p the proton magnetic moment. However, different theoretical models predict considerable deviations from the SU(6) value of $2.79\mu_N$, as illustrated for the case of the Δ^+ in Table 1. Measuring the magnetic moment therefore gives a sensitive test of the validity of the various models of the nucleon.

Some time ago it was proposed to determine the magnetic moment of the $\Delta^{++}(1232)$ by measuring the $\pi^+ p \to \gamma' \pi^+ p$ reaction [6], and the first dedicated experiment of this type was performed in the '70s [1]. Different theoretical analyses of these data produce different values for $\mu_{\Delta^{++}}$ and the Particle Data Group [7] quotes $\mu_{\Delta^{++}} = (3.7 - 7.5) \; \mu_N$, where μ_N is the nuclear magneton. SU(6) symmetry yields $\mu_{\Delta^{++}} = 5.58 \, \mu_N$.

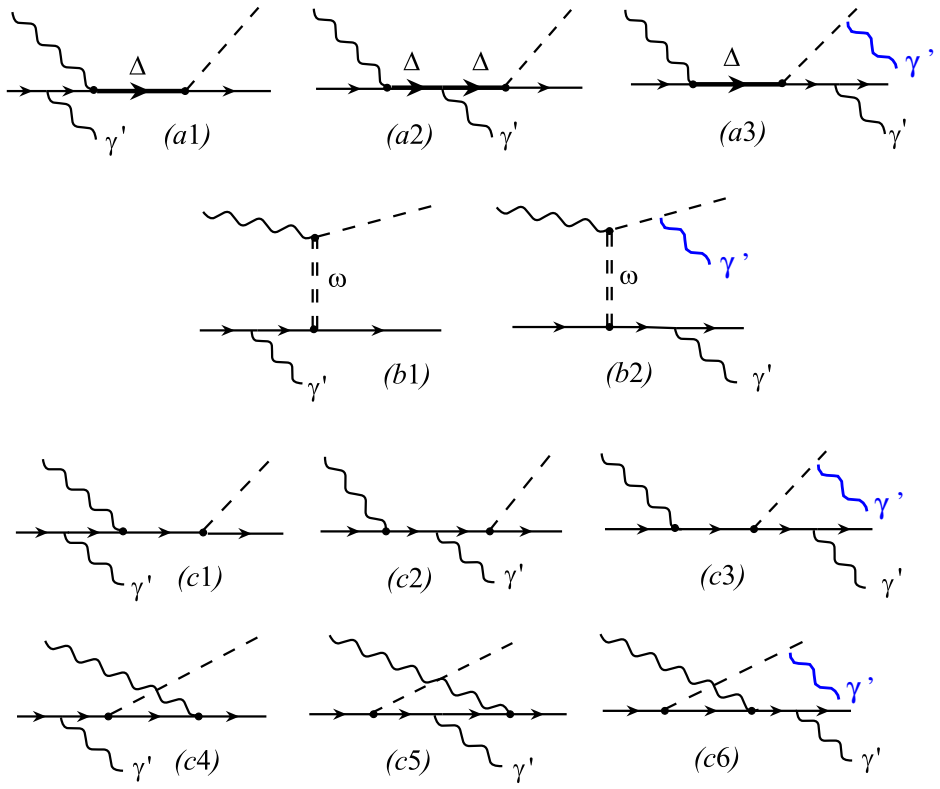

Figure 1: Feynman-diagrams for the $\gamma p \to \gamma' \pi^0 p$ reaction in the $\Delta(1232)$ region (black lines). In the case of the $\gamma p \to \gamma' \pi^+ n$ reaction the different bremsstrahlung (γ') production from the final state pion is shown by the blue lines. Solid lines represent nucleons, dashed represent pions

The large uncertainty in the extraction of $\mu_{\Delta^{++}}$ from the data is due to the model dependence of non-resonant contributions to the $\pi^+ p \to \gamma' \pi^+ p$ reaction, bremsstrahlung of the charged pion (π^+) and proton (p) and interactions between the particles in the initial and final states.

It has been proposed [8] to determine the magnetic moment of the $\Delta^+(1232)$ through measurement of the $\gamma p \to \gamma' \pi^0 p$ reaction, and calculations for this reaction have recently been performed [9, 10]. Due to the small cross sections for this reaction, which is proportional to $\alpha_{em}^2 = 1/(137)^2$, the first measurement (which demonstrated the feasibility of the method but did not yield an accurate value for $\mu_{\Delta^{++}}$) was only performed in recent years by the A2/TAPS collaboration at MAMI [5]. New experiments which will greatly improve the statistics and detector acceptance have been proposed at ELSA with the Crystal Barrel detector[13] and with the Crystal Ball detector at Mainz[14].

A detailed calculation for the $\gamma p \to \gamma' \pi^0 p$ reaction in the $\Delta^+(1232)$ region [3] has been performed using an effective Lagrangian approach. This model includes the mechanisms represented in Fig.1 which are obtained by coupling a photon in a gauge invariant way to the mechanisms which describe the $\gamma p \to \pi^0 p$ reaction in the $\Delta(1232)$ region. This yields the Δ-diagrams (a1-a3), Born diagrams where the photon is emitted from all proton lines (c1-c6), and the vector-meson (in particular ω-meson) exchange diagrams (b1-b2) which are important at the higher energies. In these calculations, the Δ-resonance is described by a pole in the complex energy plane at the position W $= (1210 - 50\,i)$ MeV. This description of the Δ intermediate state, see Fig. 1 (a1 - a3), through a pole (without an energy dependence of the pole mass and width) is important to guarantee gauge invariance [16]. In comparison with the $\gamma p \to \pi^0 p$ reaction, the description in Ref. [15] of the $\gamma p \to \gamma' \pi^0 p$ reaction invokes only one new parameter, entering due to the $\gamma\Delta\Delta$ vertex (a2). This new parameter is the Δ^+ anomalous magnetic moment $\kappa_{\Delta+}$. The Δ^+ magnetic moment $\mu_{\Delta+}$ is then obtained as: $\mu_{\Delta+} \equiv (1 + \kappa_{\Delta+})\, e/(2M_\Delta) = [(1 + \kappa_{\Delta+})\, M_N/M_\Delta]\, \mu_N$, where M_N (M_Δ) represent the mass of the nucleon and Δ respectively.

A theoretical description of the $n\pi^+\gamma'$ reaction in this effective Lagrangian approach has recently been formulated along the same lines as described for the $\gamma p \to \gamma' \pi^0 p$ reaction in [3]. The different final state

Table 1: Predictions for the magnetic dipole moment of the $\Delta^+(1232)$ state in different models

Theory	(μ_{Δ^+}/μ_N)	References
LCQCD	2.2± 0.4	T.M. Aliev *et al.*, Phys. Rev. D **62**, 053012 (2000).
QCDSR	2.19± 0.50	B.L. Ioffe, Nucl. Phys. **B188**, 317 (1981);
		F.X. Lee, Phys. Rev. D **(57), 1801 (1998).**
Latt.	2.46± 0.31	D.R. Leinweber *et al.*, Phys. Rev. D **46**, 3067 (1992).
χPT	2.1± 0.2	M.N. Butler *et al.*, Phys. Rev. D **49**, 3459 (1994).
RQM	2.38	F. Schlumpf, Phys. Rev. D **48**, 4478 (1993).
NQM	2.73	K. Hikasa *et al.*, Phys. Rev. D **45**, S1 (1992).
χQSM	2.19	H.C. Kim *et al.*, Phys. Rev. D **57**, 2859 (1998).
χB	0.75	S.T. Hong and D.P. Min, nucl-th/9909004.

particles for $n\pi^+\gamma'$ mean the background bremsstrahlung contributions to the process of interest are very different in the two reactions. The bremsstrahlung photon will be produced from the final state pion in $n\pi^+\gamma'$, rather than the final state nucleon. This pion bremsstrahlung process is stronger than for the nucleon due to the smaller pion mass. Also the Born terms (c1-c6) are stronger in $\gamma p \to n\pi^+$ than $\gamma p \to p\pi^0$[11]. This different role and strength of the various diagrams means the $n\pi^+\gamma'$ channel gives vital consistency checks of the underlying model not available from $p\pi^0\gamma'$ alone. This is important considering the unavoidable model dependence in the extraction of the magnetic moment.

Calculations of the $n\pi^+\gamma'$ cross sections based on this effective Lagrangian approach for the main Δ diagrams (a1,a2 and a3 in Fig.1) are compared with those for the $p\pi^0\gamma'$ channel in Fig 2. The stronger role of the bremsstrahlung terms in the $n\pi^+\gamma'$ channel is suggested by the larger magnitude and characteristic $\frac{1}{E_{\gamma'}}$ dependence of the cross section at lower photon energies. However, for incident photon energies in the region of the Δ resonance and for E_γ^{cm} ~100 MeV (where E_γ^{cm} is the energy of the decay photon in the cm system of the initial γp) the predicted cross sections for both reactions are of similar magnitude and both show similar sensitivity to the Δ^+ magnetic moment. These calculations are presently being improved and a unitarized simultaneous description of both $n\pi^+\gamma'$ and $p\pi^0\gamma'$ reactions including all diagrams in Fig.1 is expected to be available in the near future. These developments in theory give additional motivation for the proposed measurement as determination of more than one final state allows the systematics of these rescattering effects to be more fully tested.

The measurement of $\gamma p \to \gamma'\pi^+ n$ will use linearly polarised photons in the Δ region. At present theoretical predictions of the photon asymmetry are only available for $\gamma p \to \gamma'\pi^0 p$ as shown in Fig. 3. In this reaction the sensitivity of the differential cross section and the photon asymetry to the Δ^+ magnetic moment are predicted to be strongly enhanced by looking in kinematic regions where the role of bremsstrahlung terms is suppressed (Fig.3). Equivalent calculations for the $n\pi^+\gamma'$ channel are expected to be available shortly[2] and the possibility of obtaining increased sensitivity to the magnetic moment through kinematic cuts in the $n\pi^+\gamma'$ measurement will be explored in the near future.

3 Experiment

3.1 Equipment

The experimental setup will be the same as proposed for the $\gamma p \to \gamma'\pi^0 p$ measurement using the Crystal Ball and TAPS detector system (CBTAPS) with the Glasgow tagged photon spectrometer at MAMI.

The tagging facility at MAMI B ($E_0 \leq 855$ MeV) can tag bremsstrahlung photons in the energy range 40−800 MeV with a resolution of ~ 2 MeV at rates up to $10^8\ s^{-1}$. The system consists of a momentum-dispersed electron spectrometer, with an intrinsic energy resolution of 120 KeV [17]. This spectrometer focuses the post-bremsstrahlung electrons onto the focal plane where the position and time of arrival are established. The focal plane detector [18] consists of 353 half overlapping plastic scintillators. The overlap region between two detectors defines the energy resolution of the tagged photon beam. The maximum tagged photon flux is $\sim 10^6 s^{-1}$ per channel.

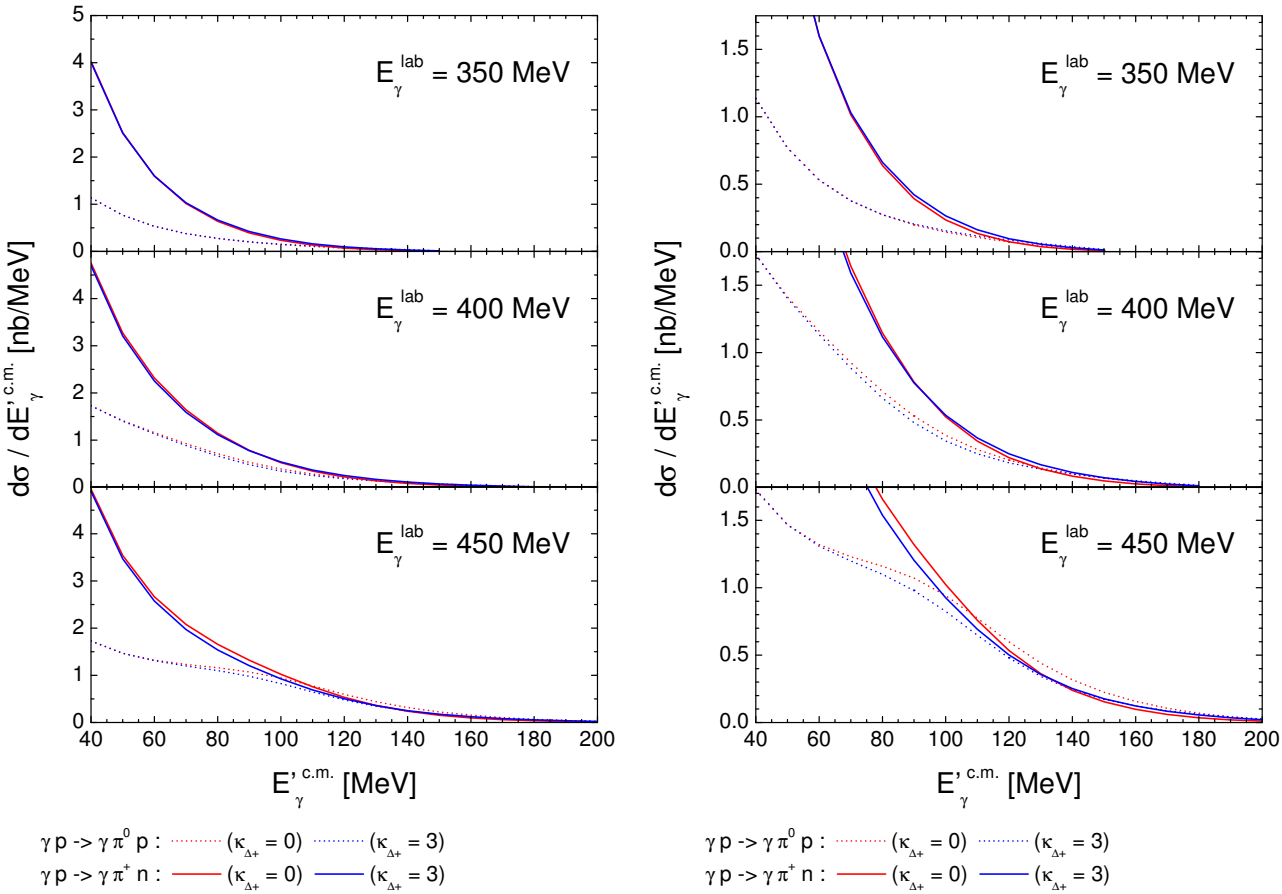

Figure 2: Energy dependence ($d\sigma/dE_\gamma^{'c.m.}$) of the outgoing photon for the $\gamma p \to \gamma' \pi^+ n$ (solid) and $\gamma p \to \gamma' \pi^0 p$ (dashed) cross sections integrated over photon and pion angles. The calculations correspond to the values : $\kappa_{\Delta+} = 0$ (red) and $\kappa_{\Delta+} = 3$ (blue). Right panel shows the same data with restricted y scale. Only Δ mechanisms are included in the calculations.

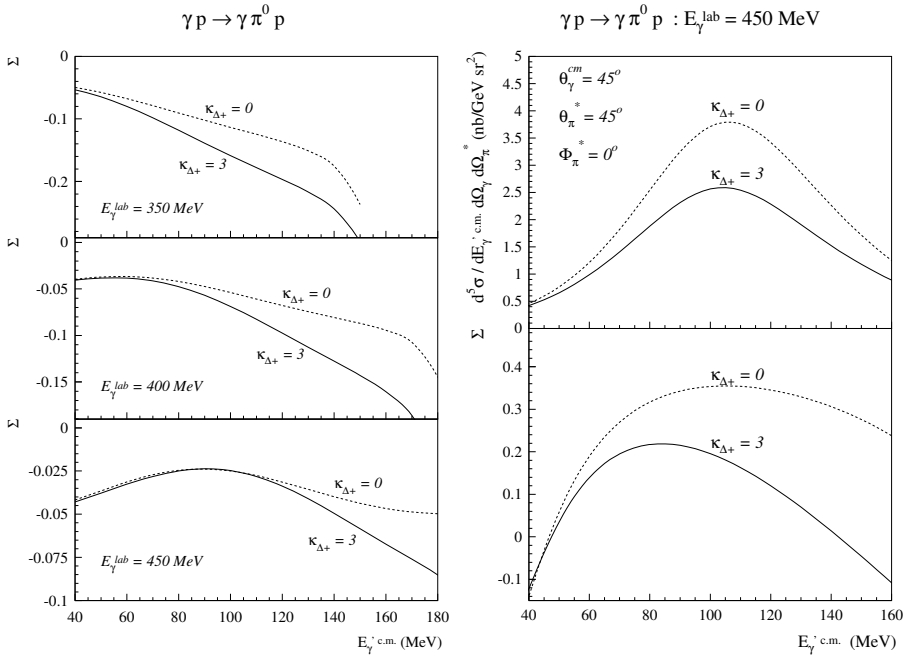

Figure 3: Left panel: The energy dependence of the asymmetry $\Sigma \equiv (d\sigma_\perp - d\sigma_\parallel)/(d\sigma_\perp + d\sigma_\parallel)$ for γ', partially integrated over the photon and pion angular range $0^o < \theta_\gamma^{c.m.} < 90^o$, $0^o < \theta_\pi^* < 180^o$, $-90^o < \Phi_\pi^* < 90^o$, and differential with respect to the outgoing photon energy $E_\gamma^{'c.m.}$. Right panel: Five-fold differential cross section $d^5\sigma$ (upper), and corresponding photon asymmetry Σ (lower) for the $\gamma p \to \gamma' \pi^0 p$ reaction as a function of the outgoing photon c.m. energy and for the restricted γ' and π angles indicated in the figure.

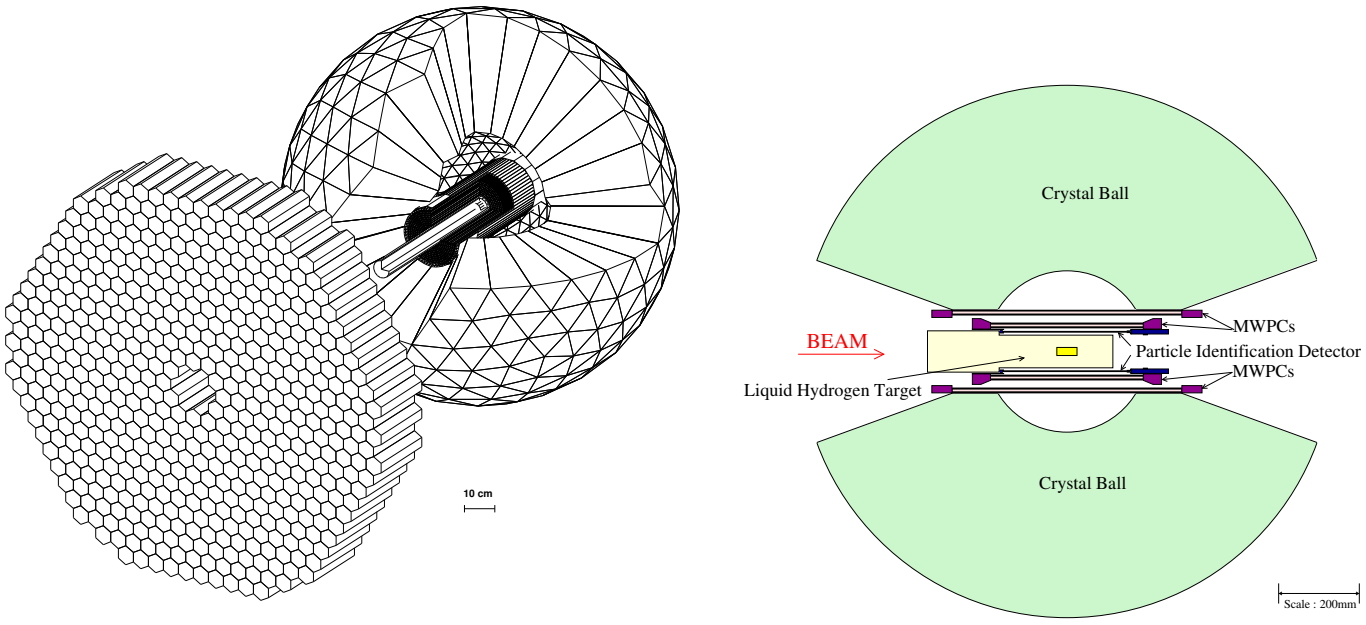

Figure 4: The experimental apparatus proposed for the measurements of $\mu_{\Delta+}$ at MAMI. Left panel: Crystal Ball and TAPS forward wall. Right panel : Section through the Crystal Ball indicating the position of the wire chambers and particle-ID detector.

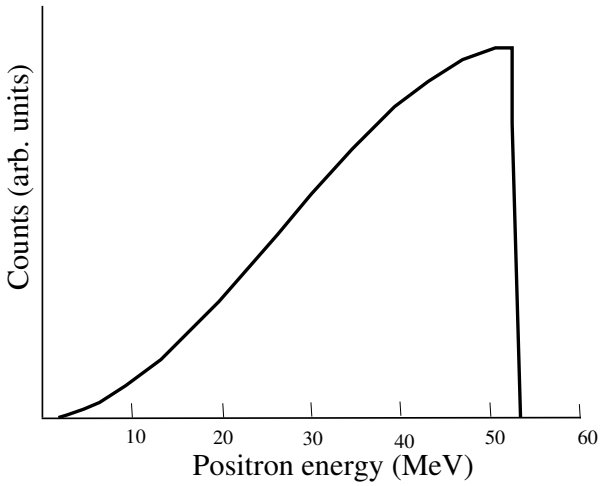

Figure 5: The Michel spectrum of positron energies from the muon decay[21]

The CB (Fig. 4) is constructed of 672 optically isolated NaI(Tl) crystals, 15.7 radiation lengths thick. The counters are arranged in a spherical shell with an inner radius of 25.3 cm and an outer radius of 66.0 cm. Each crystal is shaped like a truncated triangular pyramid, 40.6 cm high, pointing towards the center of the Ball. The sides on the inner end are 5.1 cm long and 12.7 cm on the outer end. The Ball has an entrance and exit opening for the beam which results in a loss of 4.4% of acceptance. A charged particle tracker, comprised of two coaxial cylindrical multiware proportional chambers (MWPC) developed for the DAPHNE large-acceptance tracking detector [19] will be used to give accurate angle information on the π^+. A plastic scintillator particle-identification detector (PID)[20], presently being constructed in Glasgow, will be placed between the wire chamber and the target to separate pion and proton events. Both these sub-detector systems are shown schematically in Fig. 4.

The trajectory and energy of particles for $\theta < 20°$ will be measured by the TAPS forward wall. The TAPS detector system will cover the exit (downstream) opening of the Crystal Ball. TAPS[22] is comprised of 540 individual barium fluoride (BaF_2) crystals. The crystals are hexagonally shaped with an inscribed diameter of 59 mm and a length of 250 mm (12 radiation lengths). BaF_2 has three scintillation components in the UV region, two fast ones and one slow one. The relative light yield depends on the ionization density and, therefore, allows particles discrimination by pulse-shape analysis. The fast component provides excellent timing characteristics. In front of each crystal a hexagonal plastic scintillator (NE102A) tile is mounted and read by a separate photomultiplier. This tile provides acts as a "VETO" for charged particles.

3.2 π^+ detection

The π^+ decays with a mean life of ~26ns into a μ^+ and a muon neutrino. The μ^+ generally gains little kinetic energy from the decay, only acquiring ~4.1 MeV kinetic energy in the pion rest frame. The μ^+ decays with a mean life of 2.2 μs to a positron and two neutrinos. The positrons have energies up to ~52 MeV. The energy distribution is known as the Michel spectrum[21] and is shown in Fig. 5.

The response of the CB to π^+, calculated using a GEANT3 based Monte Carlo model, is shown in Fig. 6 which shows the energy deposited by 150 MeV pions. The plot on the left shows the energy spectrum if we wait for all particle decays to occur. As expected there is little evidence of a peak at the kinetic energy of the incident pion as the energy from the π^+ decay products will also be in the ball. In fact the sharp cut off in the energy deposited at 52 MeV above the incident pion energy, due to the Michel spectrum of positron energies from the μ decay, is clearly visible. Some events deposit less than 150 MeV in the ball due to inelastic nuclear interactions of the pion with the scintillator material. The strength at the highest energies is due to pion absorption nuclear interactions eg. $(\pi, 2N)$, where the pion rest mass is available to the final state particles.

The right hand figure shows the spectrum if we wait only 1 μs. This is the approximate period over which the ADCs on the Crystal Ball will sample the NaI signals in the experiment. We now see the energy peak near

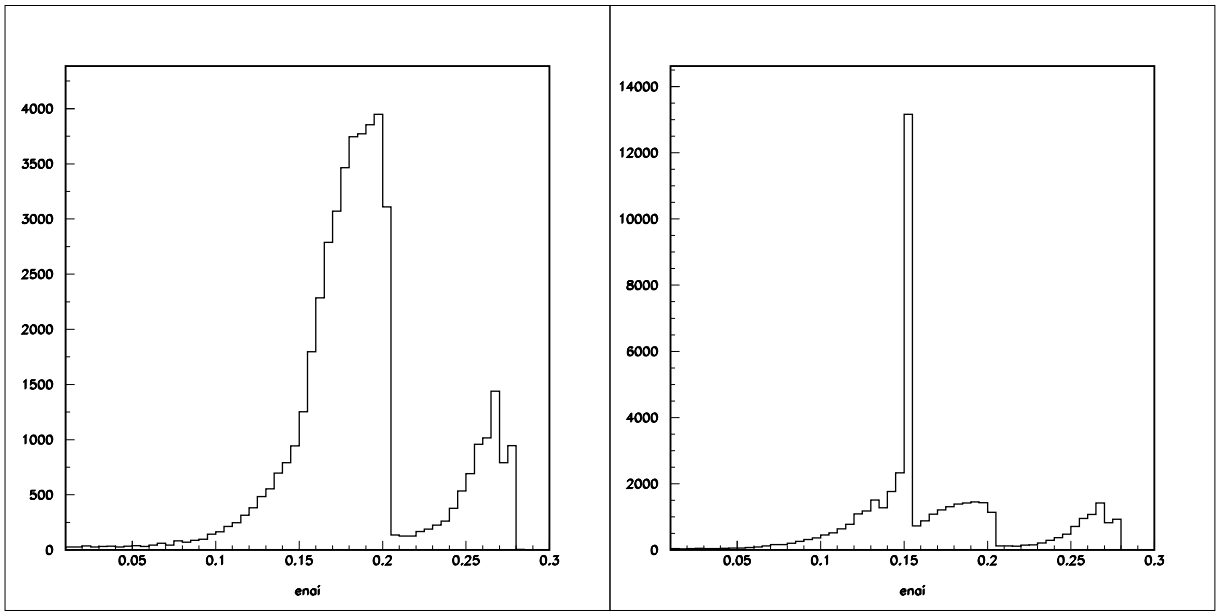

Figure 6: GEANT simulations of the energy deposited (GeV) in the Crystal Ball by 150 MeV π^+ emitted isotropically from the centre of the ball. The left panel shows the energy deposited if time is allowed for all particle decays to occur. The right panel shows the energy deposited within 1μs.

150 MeV for π^+ events which do not have an associated muon decay. There is also of course a corresponding reduction in the strength in the ~52 MeV region above the peak.

The feasibility of good energy determination for a subset of π^+ events, in a situation resembling real experimental data more closely is shown in Fig 7, where two further steps in the analysis have been taken. i) The energy deposits predicted by the GEANT simulation have been smeared by a factor consistent with the experimentally observed pulse-height resolution and ii) the output of the simulation (in event-by-event format) was then analysed with the standard cluster finding algorithms used in the Crystal Ball analysis software.

Fig.7 (left) shows the energy of the clusters with the restriction of a 1μs time gate. The energy distribution of the highest energy cluster looks similar to Fig. 6, but smeared due to the resolution effects. There are also secondary clusters found at lower energies due to split-off events created from the pions' decay or interaction. Fig.7 (right) has the additional condition that the number of crystals in the cluster with the highest energy is less than 3. This cut rejects a lot of these muon decay or pion nuclear interaction events, both of which tend to produce clusters which contain a larger number of crystals than a "clean" pion event. With these cuts a clear signal is observed close to the incident pion energy on top of a manageable background. The peak contains ~25% of the pions incident on the detector.

More detailed investigations of shower shape will be carried out when real experimental data is available and a new shower finding algorithm dedicated to π^+ detection will be developed. It may also be possible to further improve the π^+ energy determination by looking at the associated signals in the Glasgow particle-ID detector (Fig. 4).

3.3 Neutron detection

The capabilities of the Crystal Ball for neutron detection have been investigated in a measurement of the $\pi^- p \rightarrow \pi^0 n$ reaction at the Brookhaven national laboratory AGS[23]. The two body kinematics of the reaction were used to obtain energy and angle tagged neutrons with kinetic energies up to 250 MeV. The angular resolution of the Crystal Ball for detecting the tagged neutrons (Fig. 8) was found to be ~10° (FWHM). This includes the uncertainty in the neutron angle (calculated from the measured π^0 angle) and the uncertainty in the reaction vertex. The proposed experiment should have somewhat better angular resolution than the ~10° quoted.

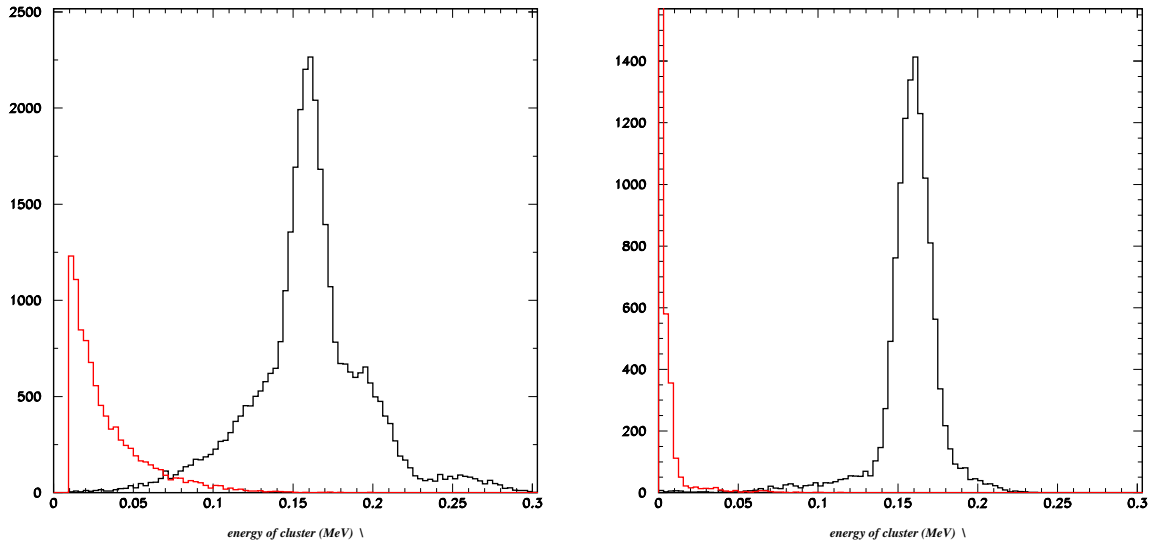

Figure 7: Energy of clusters produced in the Crystal Ball by 150 MeV π^+. The left panel shows the spectra integrated over a time period of 1μs. The black histogram shows the highest energy cluster. The red histogram shows the energies of the split off clusters. The right panel shows the same data with an additional restriction that the number of crystals in the highest energy cluster should be less than 3.

Figure 8: Left panel: Angular resolution of the Crystal Ball for neutron detection[23]. Right panels: Neutron detection efficiency with the restriction that at least one crystal in the cluster had greater than 20 MeV deposited (upper) and greater than 10 MeV deposited (lower). Solid points show experimental data. Open points show results from GEANT simulations.

The efficiency for neutron detection extracted from the experiment is shown in the right panels of Fig.8 for two different cluster energy thresholds of 20 MeV(upper) and 10 MeV(lower). The efficiency is ~30% at 100 MeV neutron energy and rises to ~40% at 250 MeV. Neutrons forward of 20° will be detected in TAPS. This has an efficiency of ~25% and the neutron energy can be measured using the time of flight.

It was found in Ref.[23] that for ~10% of neutron events a second split-off cluster is found in the Crystal Ball. We have carried out a GEANT simulation and find a similar probability for these "split-off" clusters. The secondary clusters predominantly have energies below 50 MeV.

3.4 Detection efficiencies

To measure the π^+ and neutron detection efficiencies in the detector system it will be necessary to have a source of energy and angle tagged events. It is planned to obtain these using data from the $\gamma p \to \pi^+ n$ reaction. For a fixed photon energy the reaction is completely determined below the 2π production threshold by the angle of the π^+ which will be measured accurately in the wire chambers. Test data with a proton target will be obtained in the commisioning stages of the Crystal Ball and we will analyse part of the data to check the detection characteristics and to extract detection efficiencies. Two-cluster events will also be recorded along with the proposed measurement.

3.5 Background reactions

The expected $\gamma p \to \gamma' \pi^+ n$ total cross section for decay photon energies above 50 MeV is $\sim$ 100 nb. The emitted photon energy spectrum ranges from 0 to 250 MeV. We are primarily interested in γ' with energies greater than 70 MeV where the data are predicted to show sensitivity to the Δ^+ magnetic moment. The major anticipated background reactions are

$$\gamma p \to \pi^+ n, \tag{2}$$

$$\gamma p \to \pi^+ \pi^0 n, \tag{3}$$

Reaction 2 at our incident photon energy has a total cross section of about 150 μb [24]. It will contribute to the "good" events sample due to cases where one of the particles has produced two clusters in the detector ("split-off"). In a fraction of the cases the split-off could be confused as a γ' event. GEANT simulations indicate the energies of secondary clusters from split-offs predominantly have low energies. A simple cut on the reconstructed cluster energy of ~50 MeV is predicted to suppress their contributions by over ~99%. Further significant reductions of the strength are expected when looking for the tight energy and angle correlation from the two body kinematics of the $\gamma p \to \pi^+ n$ reaction.

The two pion production processes are only important for the higher photon energies sampled in the experiment. The $\gamma p \to \pi^0 \pi^+ n$ reaction has a cross section of ~300 nb [25] at a photon energy of ~390 MeV. If one of the photons from the decay of the pion is not detected then some of the time the remaining photon could end up in the "good events" sample. The π^0 detection efficiency for the CBTAPS detector system is over 85% for much of the pion angular range which will reject most of this background. Other kinematic cuts based on invariant mass reconstruction will further suppress this process eg. the missing mass of the neutron from the assumed γ' and the π^+.

4 Event Rates

The proposed experiment will use the MAMI/Glasgow Tagged Photon beam in the MAMI A2 area.

The parameters entering the count rate estimate and resulting beam time request are:

- Incoming electron beam energy: $E_0 = 882$ MeV.
- Tagged photon energy range: $E_\gamma^t = 295 - 820$ MeV.
- Electron count rate in the tagger: $N_e = 5 \times 10^5$ s^{-1} MeV^{-1}

- Tagging efficiency: $\varepsilon_t \approx 50\%$.
- Tagged photon flux: $N_\gamma = 2.5 \times 10^5$ s^{-1} MeV^{-1}
- Number of protons in a 5 cm long LH_2 target (existing DAPHNE cryo target): $N_t = 2.1 \times 10^{23}$ cm^{-2}
- Detection efficiency: $\epsilon_{\pi+}$=$\sim$25%; $\epsilon_{neutron}$=$\sim$30%; $\epsilon_{\gamma'}$=$\sim$90%. Total efficiency ϵ_{CB} $\sim$6.75%
- Data acquisition system live time: $\varepsilon_{DA} \approx 70\%$.
- Total cross section for $\gamma p \to \gamma' \pi^+ n$: $\sigma_t \sim 100$ nb.
- Differential cross section partially integrated: $d\sigma/dE'_\gamma \sim 0.5$ nb/MeV. (see Fig.2).

The resulting number of events expected per hour per MeV of the incident photon energy and per MeV of production photons is

$$N_{\gamma'} = N_\gamma \ \frac{d\sigma}{dE'_\gamma} \ N_t \ \varepsilon_{CB} \ \varepsilon_{DA} \approx 0.008 \left[\frac{1}{MeV} \ \frac{1}{hour} \ \frac{1}{MeV}\right]. \tag{4}$$

The beam time already approved for $\gamma p \to \gamma' \pi^0 p$ is 500 hours, plus 300 hours for an engineering run plus 100 hours for empty target and background measurements. This same period will provide about 0.7×10^5 $\gamma p \to \gamma' \pi^+ n$ events integrated over the production photon energy $E'_\gamma = 30 - 150$ MeV and over a 150 MeV region between 340 and 490 MeV for the tagged incident photons.

The expected rate for the differential cross section measurement in $\pm$25 MeV incident photon energy bins and $\pm$10 MeV integral in the production photon energy is

$$N_{\gamma'} \approx 7 \left[\frac{1}{50 \ MeV} \ \frac{1}{hour} \ \frac{1}{20 \ MeV}\right]. \tag{5}$$

The photon asymmetry Σ will be measured with the coherent peak set at about 450 MeV. The linearly polarized photons cover the range between 370-450 MeV with a mean polarization $P_\gamma \approx 40\%$. The number of events expected in the 500 hours is about 0.34×10^4 per bin of $\pm$25 MeV incident photon energy and $\pm$10 MeV production photon energy. The expected accuracy in the photon asymmetry is

$$\Delta\Sigma = \frac{1}{P_\gamma} \ \frac{1}{\sqrt{N}} \approx 0.04 \tag{6}$$

per bin of $E^t_\gamma = \pm 25$ MeV and $E'_\gamma = \pm 10$ MeV.

References

[1] B. Nefkens et al., Phys. Rev. D18, 3911 (1978).

[2] M. Vanderhaegen, private communication; W.-T. Chiang *et al.*, in preparation.

[3] D. Dreschel and M. Vanderhaegen, Phys. rev.C64,065202(2001).

[4] A.I.Machavariani and Amand Faessler, arXiv:nucl-th/0202060 (2002).

[5] M. Kotulla et al. PRL 89 272001 (2002).

[6] L. A. Kondratyuk und L. A. Ponomarov, Yad. Fiz. 7 (1968) 11. [Sov. J. Nucl. Phys. 7 (1968) 82].

[7] D. E. Groom *et al.*, Eur. Phys. J. C 15 (2000) 1.

[8] Finanzierungsantrag SFB 201 (1984-86), S. 56.

[9] A. I. Machavariani, A. Faessler, and A. J. Buchmann, Nucl. Phys. A 646 (1999) 231.

[10] D. Drechsel, M. Vanderhaeghen, M. M. Giannini, E. Santopinto, Phys. Lett. B 484 (2000) 236.

[11] D. Drechsel, O. Hanstein, S. Kamalov, and L. Tiator, http://www.kph.uni-mainz.de/MAID (2000)

[12] M. Kotulla, PhD thesis, Giessen University (Germany), 2001.

[13] R. W. Gothe *et al.*, *Inelastic Photon Scattering in the Exclusive Channels* $p(\gamma\pi^0\gamma p)$ *and* $p(\gamma\eta\gamma p)$ Proposal to the ELSA/MAMI PAC (2001).

[14] R. Beck, M. Kotulla, A. Starostin *et al.* Crystal Ball collaboration, Proposal to the ELSA/MAMI PAC (2002).

[15] D. Drechsel and M. Vanderhaeghen, Phys. Rev. C 64 (2001), 065202.

[16] G. López Castro and A. Mariano, hep-ph/0010045.

[17] I. Anthony et al., NIM A 301 (1991) 230.

[18] S.J. Hall et al., NIM A 368 (1996) 698.

[19] G. Audi *et al*, Nucl. Instr. and Meth. **A301**, 473(1991).

[20] D.P. Watts, Crystal Ball collaboration meeting, www.physics.gla.ac.uk/∼dwatts/pid.html (2003)

[21] F. Scheck, Leptons, hadrons and Nuclei, (Elsevier Science Publishers B.V. 1983) p. 324.

[22] R. Novotny, IEEE Trans. Nucl. Sci. A **38**, 379 (1991).

[23] T.D.S. Stanislaus, D.D. Koetke *et al.*, Nucl. Instr. Meth. A462 (2001) 463

[24] M.McCormick et al., Phys. Rev. C 53, 41 (1996).

[25] Langgaertner et al, PRL 87 052001(2001).